Input-output relation of FitzHugh-Nagumo elements arranged in a trifurcated structure

T. Yanagita*
Research Institute for Electronic Science, Hokkaido University, Sapporo 060-0812, Japan
(Received 12 March 2007; published 28 November 2007)

In this study, the propagation of an action potential in a network of excitable elements is studied numerically. The network we consider consists of excitable elements arranged in the shape of a trifurcated structure having three cables. The system has a branch point, a Y junction, at which the three cables are joined. Two types of external stimulations are considered: a single impulsive stimulation at one of the cable terminals, and a pair of stimuli applied to two different terminals. We have found three basic phases depending on the excitability of the elements for a single external stimulus as follows: (1) signal distributor—as the excitability gets higher, the pulse generated by a stimulus splits into two at the branch point, and two pulses are transmitted to the opposite terminals, (2) propagation block—the pulse in the lower excitable chain is blocked at the branch point, and (3) transient propagation—as the excitability is decreased further, we see that the pulse vanishes before reaching the branch point. By the interaction between the pulses that originate from different sources, signal transmission is recovered if the pulses arrive at the branch point nearly synchronously or after a specific delay time. The effects of the repetition of these two types of stimulation are also investigated. Complex spatiotemporal patterns occur due to pulse-pulse interaction and collisions at the branch point. The input-output relationship, which depends crucially on the repetition period and the time lag between the pair of stimuli, is characterized by the stimulus-response ratio and the interspike interval. We also show the effects of noise on the distribution of the interspike interval.

DOI: 10.1103/PhysRevE.76.056215 PACS number(s): 05.45.−a, 82.40.Bj, 75.40.Mg

I. INTRODUCTION

From the time the work of Hodgkin and Huxley [1] first appeared, and after the basic mathematical model by FitzHugh and Nagumo [2,3] was developed, the number of research reports on the subject of excitable elements has increased enormously. It is well known that excitability is a key property of many physical systems and plays a fundamental role in neural information processing as well as many other biological systems. For a simple excitable element, a small but finite perturbation to a rest state leads to a large excursion (an excitation). The excitation of a single element has been successfully modeled by ordinary differential equations. This excitation is associated with an action potential (AP) in a nerve or heart tissue.

Repetitive stimulations to a single neuron show a variety of response patterns [4–6]. For spatially extended excitable systems, it is known that a localized stimulus of a finite amplitude forms a stable propagating pulse. Instabilities and entrainment of propagation originating from a pulse-pulse interaction in an excitable medium have been reported in [7–9]. It is also shown that repetitive localized stimuli show exotic behaviors, e.g., propagation failure and resonance phenomena [10]. Thus, spatial degrees of freedom might play a crucial role in determining the dynamical behavior and information processing in a neuronal system.

Most neurons have complicated shapes, particularly bifurcation patterns in dendrites and axon terminals. Specifically, dendrites tend to bifurcate repeatedly and create a (often several) large and complicated tree. A particular dendritic morphology behaves as a complex dynamical device with potentially rich repertoires of input-output capabilities [11–14]. Here, the branch point (the junction) of cables might play a crucial role in determining the pulse propagation on a dendritic tree. Thus, single-element models are too simple to allow the activity on an actual neuron to be studied. In fact, an AP can either completely fail to propagate beyond the branch or succeed in propagating beyond the branch point [15,16].

Mathematical models for aiding the exploration of the physiological implications of dendritic branching have been developed over the past decades [12,13,15,17]. The concept of "impedance mismatch" is an important result of the theoretical studies [15,16]. When an AP propagates toward a region with a geometrical change (e.g., a branch point), the propagation of the AP near this point will continue unperturbed if the impedance load in front of the AP remains as in a uniform cylinder. If, however, the impedance at the geometrical change is smaller than that in the parent cable, the AP will suffer a larger current sink from the regions beyond the geometrical change and both its velocity and amplitude will be reduced as it approaches the geometrical change. When such an impedance mismatch is moderate, the AP will succeed in actively propagating (after some delay) beyond the branch point, and it will regain its original shape and velocity. For a sufficiently large impedance mismatch, however, the AP will completely fail to propagate beyond the branch point (propagation block).

The effects of geometrical changes in passive cables have been extensively studied through cable theory. However, multiple APs originating from different sources will propagate in a branch tree simultaneously. APs will interact with or collide in the vicinity of a branch point. Particular combinations of input patterns in time and space might play crucial roles in the interaction; this depends on whether APs origi-

*yanagita@nsc.es.hokudai.ac.jp;
URL: http://www-nsc.es.hokudai.ac.jp/~yanagita

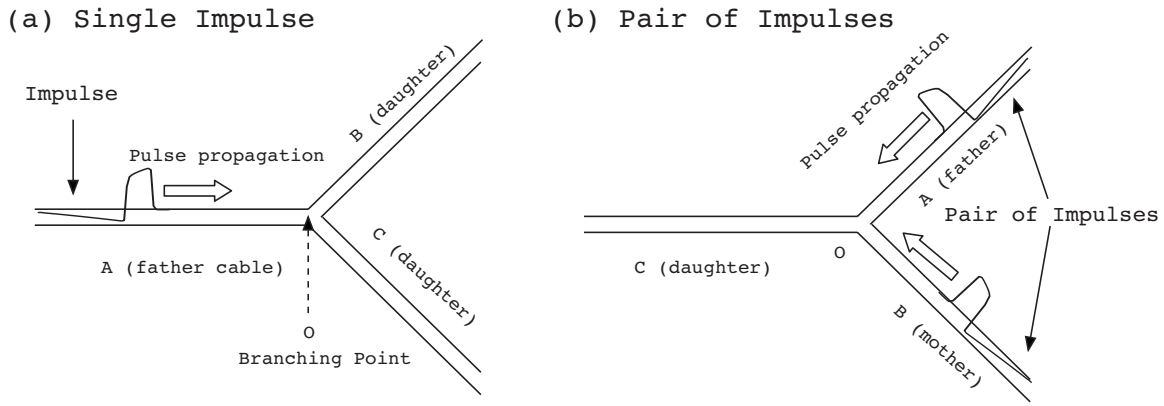

FIG. 1. Trifurcated structure consisting of three one-dimensional cables, i.e., Y-junction cables, is shown schematically. The excitable elements are aligned on the cable, as shown in Fig. 2. (a) By a single impulsive stimulus applied to the terminal of cable A, a pulse is formed and propagates in the thin cable. (b) A pair of impulsive stimuli with a time delay is applied to both terminals of cables A and B. Two pulses are generated by the pair stimuli. These dynamical behaviors depend crucially on the timing of the stimulation.

nating from different sources arrive at a branch point synchronously, or nearly so. Although a real neuron has a complicated tree structure and local dynamics, it is important to study how a simple geometrical change influences the AP propagation in response to the temporal properties of afferent impulses. In this paper, we consider an active cable with a geometrical change. A simple branch point might be a Y junction, at which three cables are joined. Here, we analyze a mathematical model consisting of three thin cables connected to each other at a branch point. Each cable is represented as a chain of excitable elements and they are connected to form a Y junction, as depicted in Fig. 1. By stimulating the terminal(s) of cable(s), we numerically explore the effect of the branch point on spatiotemporal patterns in the array of FitzHugh-Nagumo (FHN) excitable elements. All geometrical changes occur at one point (the branch point), and all the specific electrical properties are uniform over the whole structure. It is also assumed that the branch point is electrically distant from any boundary effects (i.e., all branches have constant parameters, and all terminals are sufficiently far from the branch point). Furthermore, the distance between the elements is sufficiently small as compared to the width of the propagating pulse in the cable.

When we stimulate one of the terminal nodes, i.e., the input node, by a single impulse, an excitation occurs, and then a pulse forms and propagates in the father cable. Depending on the excitability of elements, the pulse can either completely fail to propagate beyond the branch, or succeed in propagating beyond the branch point to two daughter cables. The following three phases are found depending on the excitability of elements. (i) *Signal distributor*—the pulse propagates in the father cable and reaches the branch point. Then it splits into two, and reaches the opposite terminals of the daughter cables for higher excitability. (ii) *Propagation block*—the propagating pulse is blocked at the branch point and cannot surmount it. (iii) *Transient propagation*—for lower excitability, the pulse propagates transiently in the father cable and vanishes before it reaches the branch point.

If the AP propagating from the father cable surmounts the branch point and this leads to the excitation of the opposite terminal, we regard the excitation as an output signal. The time interval between the excitations of input and output nodes, i.e., the elapsed time, depends on the excitability of the elements. The elapsed time increases as the excitability decreases and takes a maximum in the vicinity of the boundary between the signal-distributor and propagation-block phases. The branch-point-induced delay is also found in the compartment model [18,19].

The time sequence of output signals depends significantly on the repetition period when successive stimuli are applied to the input node. Because the model includes spatial degrees of freedom, the dependence of the output signals on the repetition period originates from an interaction between successive pulses propagating in the cable. Although a single pulse fails to propagate in the propagation-block phase, the repetitive stimulation leads to it surmounting the branch point. This signal transmission, however, occurs only for specific repetition periods. Thus, the system can act as a band-pass filter.

Even if the pulse generated by a single impulse vanishes at the branch point in the propagation-block phase, transmission of input signals is observed when the two terminals of the cables are stimulated. This transmission occurs only for the pair of input impulses with shorter time lags. For longer time lags, the propagation of the pulses is blocked at the branch point. More precisely, the input signal is transmitted to the daughter cable when the time lag is integer multiples of the intrinsic period of the excitable elements [10,20]. This means that the simple trifurcated array of the excitable elements acts as a coincidence detector.

The repetition of the pair of impulses also leads to complex spatiotemporal behaviors. Both the repetition period and the time lag between the pair impulses affect the input-output relation. Since the time lag between the pair of impulses is sufficiently short, the input signal is transmitted to the output node in the propagation-block phase. However, the repetition of the pair of impulses leads to transmission of the input signal to the output node even if the pulses cannot surmount the branch point for larger time lags.

We also discuss the effect of aperiodic stimulation on the input-output signal relationship. Here, the aperiodicity is

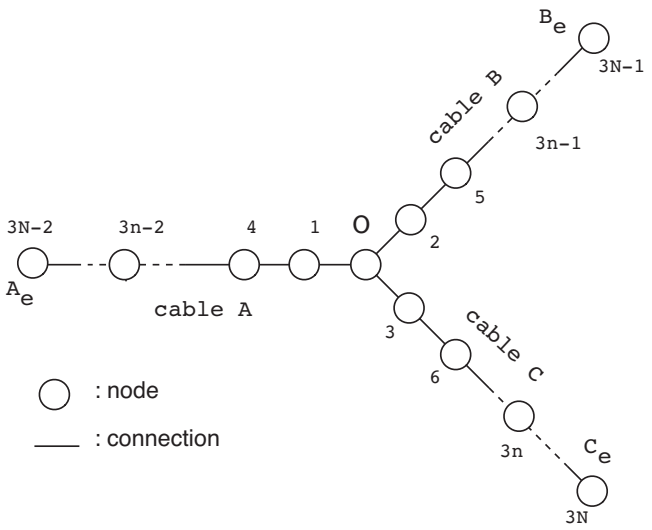

FIG. 2. The excitable system with the trifurcated structure is approximated by FHN elements arranged on the cables. At each node, we settle one FHN excitable element. Each element is coupled diffusively with its neighbors. A_e, B_e, and C_e denote the terminal nodes, where the input and the output signals are either applied or detected.

simply introduced as follows: the time intervals between successive impulsive inputs are randomly distributed around the mean interval, and the fluctuation is assumed to be Gaussian white noise. Since the fluctuation is smaller, the distribution of the interspike intervals (ISIs) of the output node shows a multimodal form. However, the unimodal distribution is obtained for larger fluctuations. Furthermore, when the mean interval of successive stimuli is approximately matched with a characteristic time scale of the excitable element, a reduction is observed in the case of the fluctuations of the time intervals between output signals.

The paper is organized as follows. A simple mathematical model, i.e., a chain of excitable elements aligned on a trifurcated structure, is introduced in Sec. II. The response to a single input impulse on the output node is discussed in Sec. III A. The propagation delay induced by the branch point is studied in Sec. III B. Section III C describes the response to the repetition of impulses. The relation between input and output signals under a pair of external stimuli is shown in Sec. III D and that under a repetition of the pair of impulses is described in Sec. III E. The effect on the output signals of fluctuation in the time interval between successive input impulses is presented in Sec. III F. Section IV concludes the paper with a brief summary and some discussion.

II. MODEL

The model considered here is a chain of excitable elements arranged in a trifurcated structure, as depicted in Fig. 2. The chain of elements, each of which is connected to its neighboring nodes diffusively, represents an excitable cable in which a pulse can propagate. The diffusive coupling is considered as a Eulerian discretization of a Laplacian, that is, the general discretization scheme for one or more parabolic partial differential equation(s) [PDE(s)] defined on an interval. At the branch point O (see Fig. 2), it is natural to introduce the diffusive coupling $u_1+u_2+u_3-3u_0$, where u_0 is the state value of the element at the branch point O, and u_1, u_2, and u_3 represent its neighboring elements. At this branch point, the membrane potential is continuous and the current should be conserved. Indeed, the diffusive coupling conserves the quantity. In other words, if a system is a network that consists of a finite number of elements and connecting nodes, then it can be regarded as a topological graph, and the Kirchhoff law must hold at each node [21]. Our model is a special case of such a topological graph system, and it has only one singular point, the branch point. The model equations are

$$\tau\frac{d}{dt}u_{3n-i} = f(u_{3n-i},v_{3n-i}) + \epsilon^2(u_{3(n+1)-i} + u_{3(n-1)-i} - 2u_{3n-i}),$$

$$\frac{d}{dt}v_{3n-i} = g(u_{3n-i},v_{3n-i}),$$

$$\tau\frac{d}{dt}u_0 = f(u_0,v_0) + \epsilon^2(u_1 + u_2 + u_3 - 3u_0),$$

$$\frac{d}{dt}v_0 = g(u_0,v_0),$$

$$u_{-2} = u_{-1} = u_0, \quad i = 0,1,2 \text{ and } n = 1,\ldots,N, \tag{1}$$

where $f(u,v)=u(u-\alpha)(1-u)-v$ and $g(u,v)=u-\gamma v$ are FitzHugh-Nagumo-type reaction functions [3,22], and α, ϵ, γ, and τ are parameters. The variables u_i and v_i correspond to the activator and inhibitor, respectively. The number of excitable elements is $3N+1$. For the terminals of every cable, we assume the following no-flux boundary conditions: $u_{3(N+1)-i}=u_{3N-i}$, $i=0,1,2$. The model can also be expressed in the following matrix form:

$$\tau\frac{d}{dt}\vec{u} = \vec{f}(\vec{u},\vec{v}) + \epsilon^2\begin{pmatrix} -3 & 1 & 1 & 1 & 0 & 0 & 0 & 0 & \cdots \\ 1 & -2 & 0 & 0 & 1 & 0 & 0 & 0 & \cdots \\ 1 & 0 & -2 & 0 & 0 & 1 & 0 & 0 & \cdots \\ 1 & 0 & 0 & -2 & 0 & 0 & 1 & 0 & \cdots \\ 0 & 1 & 0 & 0 & -2 & 0 & 0 & 1 & \cdots \\ & & \vdots & \vdots & \vdots & & & & \end{pmatrix}\vec{u}, \tag{2}$$

$$\frac{d}{dt}\vec{v} = \vec{g}(\vec{u},\vec{v}), \tag{3}$$

where $\vec{u}=(u_0,\cdots,u_{3N+1})$, $\vec{v}=(v_0,\cdots,v_{3N+1})$, $\vec{f}(\vec{u},\vec{v})=(f(u_0,v_0),\cdots,f(u_{3N+1},v_{3N+1}))$, and $\vec{g}(\vec{u},\vec{v})=(g(u_0,v_0),\cdots,g(u_{3N+1},v_{3N+1}))$. The behavior of pulse propagation in the chain is qualitatively the same as that in the one-dimensional FHN partial differential equation, that is, the Laplacian can

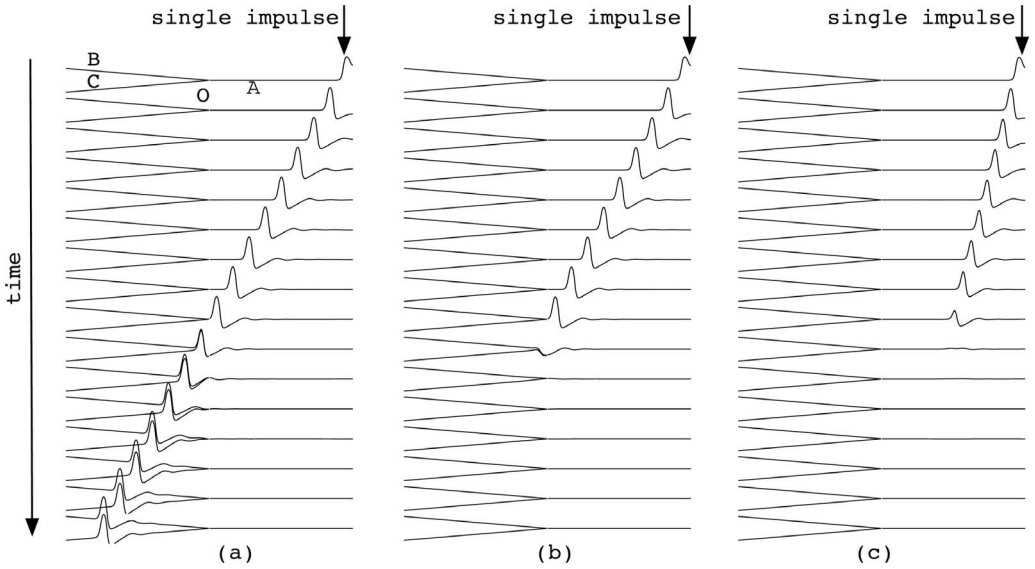

FIG. 3. Typical time evolutions of the solitary pulse generated by a single impulse. The parameters are $\epsilon=1.0$, $\gamma=1.0$, and $\tau=0.017$. (a) Distributor: $\alpha=0.002$; the solitary pulse surmounts the branch point O and propagates in the daughter cables B and C. (b) Propagation block: $\alpha=0.005$; the solitary pulse propagates in the father cable and vanishes at the branch point. (c) Transient propagation: $\alpha=0.017$; the pulse propagates transiently and disappears before it reaches the branch point.

be discretized with a nearest-neighbor approximation. A stimulus to the terminal node $3N-2$ leads to the generation of a pulse that propagates in the cable with the parameters ($\alpha=0.001$, $\gamma=1$, $\tau=0.017$). The significant difference between the model and the one-dimensional FHN PDEs is the existence of a branch point O which has three neighboring nodes. Therefore, even if the pulse propagates stably in a cable, i.e., a one-dimensional chain of excitable elements exists, whether the pulse can surmount the branch point depends on the system parameters. Furthermore, the relation between the input and output signals depends on the type of stimulation: a single impulse, a pair of impulses, or successive impulses. In the following sections, we numerically investigate the dynamical behavior of pulses and characterize their input-output relation.

When one of the terminal nodes, e.g., A_e, is stimulated, we refer to cable A as the "father" and the other cables, B and C, as "daughters" [see Fig. 1(a)]. Similarly, when two terminals A_e and B_e are stimulated, we refer to cables A and B as "parents" and cable C as "daughter" [see Fig. 1(b)]. We call the terminal(s) of the daughter(s) output node(s), and refer to the terminal(s) where the external impulse(s) are applied as input node(s).

III. SIMULATIONS

Throughout this paper, we employ a parameter region in which the FHN element is excitable (the element does not show spontaneous oscillation). The parameters are fixed as $\epsilon=1.0$, $\gamma=1.0$, and $\tau=0.017$, and we mainly investigate the dynamics of pulse propagation by changing the excitability parameter α. For external inputs, we consider that two types of impulsive stimulation are applied to the terminal node(s), and all the other elements are set to the rest state; $(u_i, v_i) = (0,0)$ for $i=1,\ldots,3N+1$. There are 601 elements, i.e., each chain is represented by 200 FHN elements.

A. Response to a single impulse

We first investigate the response to a single impulse that is applied to one of the cable terminals, i.e., the state values $u_{3N-2}(0)$ and $v_{3N-2}(0)$ are initialized to u_0 and v_0, respectively. We fix the strength of the stimulus as $u_0=1.0$ and $v_0=0.0$. Since α is smaller (excitability is higher), a solitary pulse is generated rapidly, and if the diffusive coupling parameter ϵ is suitably chosen, it propagates in the cable and reaches the branch point. Three types of behavior are found depending on the parameter α. (i) *Signal distributor*: The solitary pulse splits into two pulses, each of which propagates in the daughter cables, i.e., cables B and C, and reaches the output nodes. In this case, the input signal is transmitted to the output nodes B_e and C_e. (ii) *Propagation block*: The solitary pulse propagating from the input node disappears at the branch point. (iii) *Transient propagation*: A stable solitary pulse is not formed. The pulse propagates transiently and disappears before it reaches the branch point O.

In Fig. 3, the sequences of snapshots of the spatial pattern are depicted for different values of α. Since excitability is higher for smaller α, the solitary pulse surmounts the branch point and splits into two pulses, each of which propagates in one of the daughter cables B and C. Then, both pulses finally reach the output nodes B_e and C_e with the following parameters: $\alpha=0.01$, $\epsilon=1.0$, $\gamma=1.0$, $\tau=0.017$, and $N=200$. The excitable elements arranged in a trifurcated structure act as the signal distributor with these parameters [see Fig. 3(a)]. In general, the diffusion of the activator suppresses the excitation. Further, the effect of the diffusion of the activator at the branch point u_0 is effectively larger than that at the other node resulting from the existence of three neighboring nodes

u_1, u_2, and u_3. Therefore, the solitary pulse cannot surmount the branch point [Fig. 3(b)]. The signal is blocked and cannot be transmitted to the output nodes. As α increases further, the solitary pulse no longer propagates stably in the father cable. The pulse propagates transiently and eventually disappears before it reaches the branch point. It is well known that an isolated pulse undergoes a saddle-node bifurcation above a certain threshold value of α [23,24]. The collision of a stable pulse branch with an unstable pulse branch occurs at the saddle-node point. The saddle-node bifurcation can be intuitively understood if we consider the activator pulse as a heat source (not unlike a fire front in a bushfire). The width of the pulse decreases with increasing α because the excitability of the element is lower. Hence, the heat contained within the pulse decreases. At a critical width, or critical α, the heat contained within the pulse is too small to ignite the element in front of the pulse.

To characterize these behaviors, we calculate a signal propagation distance. Here, we regard the element i as excited nodes if $u_i(t)$ exceeds $u_c=0.5$ for any $t>0$. The signal propagation distance can be defined by

$$D = \max_{i \in M} d(A_e, u_i),$$

$$M = \{ i | \exists t \{ (t > 0) \wedge [u_i(t) > u_c] \} \}, \tag{4}$$

where M is a set of indices of the excited nodes, and $d(\cdot)$ represents the distance between two nodes. D measures how far the input signal is transmitted. The measurements of D as a function of the excitability threshold α shown in Fig. 4(a) display the existence of three phases clearly. The plateau $\alpha \in [0, \alpha_1 \simeq 0.0028]$ corresponds to a complete signal transmission, that is, the pulse generating at A_e propagates and reaches the output nodes B_e and C_e. Because we represent each cable as a chain of 200 FHN elements, the maximum distance between any two nodes is 400. For intermediate values of $\alpha \in [\alpha_1, \alpha_2 \simeq 0.0168]$, it is observed that the signal is blocked at the branch point, i.e., the pulse entering the branch point recedes and disappears. The signal propagation distance for lower excitability, $\alpha > \alpha_2$, depends on α. In this case, the pulse propagates transiently in the father cable, and the propagated distance decreases with increasing α.

Figure 4(b) shows the propagation distance in an (α, ϵ) parameter space. When ϵ is smaller, the pulse is not elicited because the single stimulus to one terminal element is not sufficient to induce excitation. It is also observed that suprathreshold excitation is not elicited for larger diffusive coupling ϵ. As a result, distributor, propagation-block, and transient-propagation phases are observed only when ϵ is an intermediate value, as shown in Fig. 4(b). In the following section, we investigate the parameter region in which these three phases exist.

B. Branch-point-induced propagation delay

It is known that local geometrical inhomogeneities produce extra delay in the pulse propagation [13,18]. The branch point is an additional source in the delay of signal transmission when α is below a critical value α_1. Our system

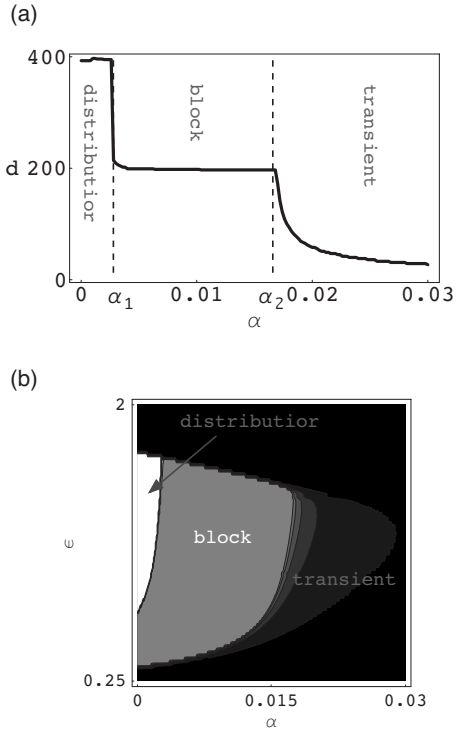

FIG. 4. (a) α dependence of the propagation distance for the solitary pulse elicited by the single impulse. The plateau in the region $\alpha \in [0, \alpha_1 \simeq 0.0028]$ corresponds to the distributor phase. However, the pulse is blocked at the branch point for $\alpha \in [\alpha_1, \alpha_2 \simeq 0.017]$. For $\alpha > \alpha_2$, the pulse propagates transiently and disappears before it reaches the branch point. (b) Propagation distance in (α, ϵ) parameter space. The white and light-gray regions correspond to $D=400$ (distributor phase) and $D=200$ (propagation block), respectively. The dark-gray region shows transient propagation. The action potential is not elicited in the black region. The other parameters have the same values as in Fig. 3.

also shows that the elapsed time, i.e., how long a solitary pulse generated at the father terminal takes to reach the daughter terminals, becomes longer with increasing α. This is caused because, when the excitability of the medium decreases with increasing α, the critical strength of the external stimulus that can lead to the excitation of the FHN element will become larger. The pulse propagating from the father cable acts as the stimulus for generating the excitation of the element at O, and the large excursion takes a longer time in the vicinity of the critical strength. In Fig. 5, the elapsed time as a function of the parameter α is depicted. The local propagation delay introduced at the branch point shows nonlinear dependence on α, and the elapsed time increases with α. For $\alpha > \alpha_1$, the propagation block is observed, i.e., the pulse entering the branch point decays and disappears at the branch point.

C. Response to the repetition of a single impulse

The repetition of a single impulse to A_e, i.e., the node $3N-2$, leads to an exotic spatiotemporal behavior. We consider the following impulsive stimulation at the node A_e:

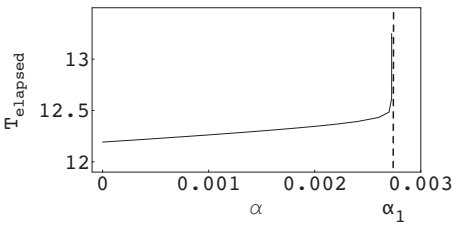

FIG. 5. α dependence of elapsed time is shown. Because a larger value of α results in lower excitability, the pulse takes a longer time to surmount the branch point, at which the effective diffusion of the activator is larger. The function shows nonlinear dependence on parameter α, and it takes larger values in the vicinity of α_1. The parameters have the same values as in Fig. 3.

$$u_{3N-2}(t_i) = u_0,$$

$$v_{3N-2}(t_i) = v_0, \tag{5}$$

where t_i is a sequence of times defined by

$$t_i \in \mathcal{T}, \quad \mathcal{T} = \{ t_n | t_n = nt_s, \ n \in \mathcal{N} \}, \tag{6}$$

where t_s is the repetition period. A pulse train is generated by the sequence of impulses. In the propagation-block phase, each pulse propagates in the father cable until it reaches the branch point, and disappears there if the repetition period is sufficiently longer. However, the spatiotemporal behavior becomes more complex for the repetitive stimulation because of the effect of interaction among the pulses propagating in the cable [10]. The input-output relation—whether the periodic stimulation leads to excitations of the output nodes—crucially depends on the repetition period.

To characterize this response to periodic stimuli, the stimulus-response ratio (SRR) has been used [4,5,10,25]. For reaction-diffusion systems on a graph, we introduce the SRR as the ratio of the number of excitations of the output node B_e to the number of stimuli. Figure 6 depicts the SRR for three phases, the signal distributor, propagation block, and transient propagation, as a function of t_s. Since the distances between the pulses generated by successive stimuli are longer for $t_s \gg 1$, the spatiotemporal behavior for periodic stimuli is essentially the same as that for the single impulse. Indeed, the SRR in the signal distributor phase equals 1 for $t_s > 3.8$ [see Fig. 6(b)]. This means that each stimulus generates a pulse that propagates until it reaches the output nodes, i.e., two terminals of the daughter cables B_e and C_e excite every stimulus cycle. When the phase is a propagation block or transient propagation, the SRR equals zero for longer t_s, that is, all pulses vanish before reaching the output nodes [Figs. 6(b) and 6(c)].

The spatiotemporal behaviors of successive pulses for larger t_s are consistent with those obtained in the case of the single impulsive stimulus as described in the previous section. However, an unexpected input-output relationship emerges for shorter repetition periods. For the signal-distributor phase, there are regions of repetitive periods, $t_s \in [1.5, 2.1]$, $[1.85, 2.05]$, $[2.55, 2.95]$, and $[3.4, 3.6]$, where the SRR in Fig. 6(a) is smaller than 1. The interference between the preceding and posterior pulses is developed in these repetition-period regions. As a result, the signal transmission is suppressed, and it is observed as a sudden decrease in the SRR in Fig. 6(a). In contrast, the repetitive stimulation with suitable periods leads to the propagation of signals beyond the branch point even if the solitary pulse is blocked at the branch point: the repetition-period regions are $t_s \in [0.95, 1.65]$, $[1.85, 2.35]$ $[2.55, 3.05]$, and $[3.45, 3.85]$ in Fig. 6(b). Furthermore, even in the case of the transient-propagation phase in which the solitary pulse vanishes before it reaches the branch point, a suitable periodic stimulation leads to the transmission of input signals [Fig. 6(c)]. Several observations mentioned in the last few paragraphs indicate that we can enhance or suppress the signal transmission by tuning the repetition period. The enhancement or

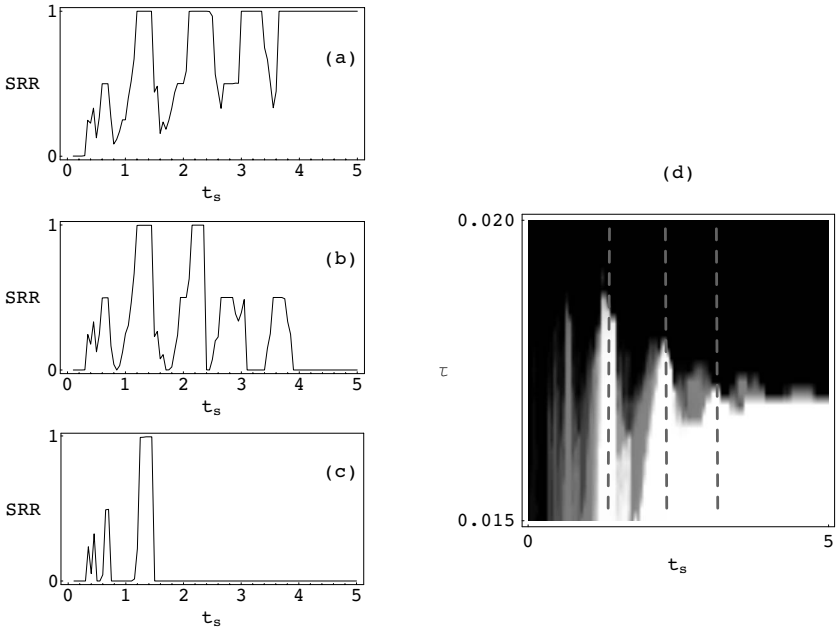

FIG. 6. Series of SRRs as a function of the repetition period. When the stimulus period has a suitable value, the pulse train can propagate until it reaches the output nodes {corresponding to the plateau near $t_s = [1.2, 1.5]$ in (b) and (c), for example}, even if a solitary pulse cannot propagate stably. (a) The signal-distributor phase: $\alpha = 0.002$. (b) The propagation-block phase: $\alpha = 0.005$. (c) The transient propagation phase: $\alpha = 0.017$. (d) The SRR in (t_s, τ) parameter space is shown by a gray scale; the maximum value of 1.0 corresponds to white, and the minimum value 0.0 to black. The broken lines indicate the times at which subthreshold excitations occur after a suprathreshold excitation. The other parameters have the same values as in Fig. 3.

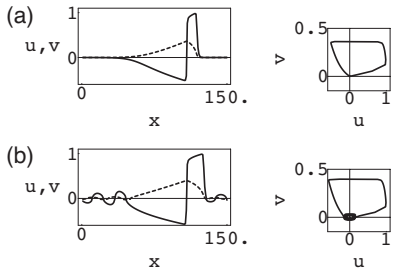

FIG. 7. Spatial profile and phase plane plot for monotonic and oscillating wake pulses propagating in a one-dimensional cable under periodic boundary conditions. To observe the tiny oscillating wake, we have used the transformation $f(x)=\mathrm{sgn}(x)|x|^{1/2}$ for u and v. In the spatial patterns (left side), the full (dotted) line indicates the profile of $f(u)$ $[f(v)]$. $\epsilon=1.0, \gamma=1.0, \tau=0.017$. (a) Monotonic wake pulse, $\alpha=0.1$; (b) oscillating wake pulse, $\alpha=0.002$.

suppression structure in (t_s, τ) parameter space is shown in Fig. 6(d).

It is known that there are two qualitatively different pulses [26], i.e., a pulse that has a monotonic wake and one that has an oscillating wake (see Fig. 7 for the typical spatial profile of these cases). Subthreshold oscillations are formed in the wake of suprathreshold excitation. As shown in Fig. 7(b), the oscillating wake comprises small successive humps behind the suprathreshold excitation. The parameter values used here admit the oscillating wake, and it is known to produce exotic behavior [10,20,27–29]. Further, it has been shown that the suppression and enhancement of signal transmission is a result of interference between the preceding and posterior pulses through the "oscillating wake" of the traveling pulse [10].

When the repetition period is shorter, more than one pulse travels in the cable, and a posterior pulse will be affected by the oscillating wake of the preceding one. Further, the effect of the wake is excitatory or inhibitory depending on the distance between pulses (the schematic illustration is shown in Fig. 8). By the interference between pulses, exotic behaviors, i.e., the so-called resonance and propagation failure [10], emerge in the following manner. When the position of the primary hump of the preceding pulse coincides with that of the supraexcitation of the posterior pulse, the preceding pulse affects the posterior pulse excitatory (see Fig. 8 for a schematic explanation). Consequently, the wake of the preceding pulse supports the propagation of a posterior pulse, and the pulse train travels stably in space even if the solitary pulse generated by a single impulse vanishes before reaching the branch point. In the case of the suppression of signal transmission, a sudden decrease in the SRR is observed, as depicted in Fig. 6(a), and the corresponding spatial profile of traveling pulses is shown schematically in Fig. 8(c).

For a trifurcated structure, the propagation block results from a local inhomogeneity, and, further, the repetitive stimulation affects the spatiotemporal behavior. To characterize statistical changes in input-output relationships, we calculate the probability density of the interspike interval, which is defined as follows. We define a sequence of times $\mathbb{T}$ at which excitations of the output node of daughter cable A_e occur as follows:

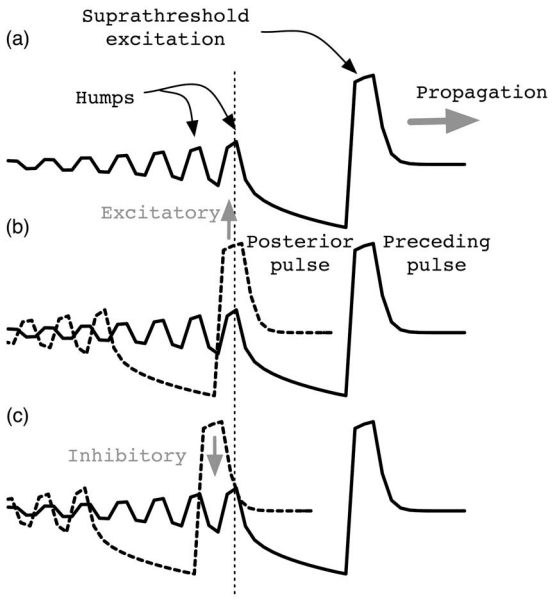

FIG. 8. Interaction between successive pulses propagating in a cable shown schematically. The interaction between pulses is excitatory or inhibitory depending on the distance between them. (a) Spatial profile of solitary pulse with an oscillatory wake. The subthreshold oscillation exists behind the suprathreshold excitation (subthreshold humps are magnified for clarity). The dotted line represents the position of the first subthreshold excitation of the preceding pulse. (b) When the position of the primary hump of the preceding pulse (the solid curve) coincides with that of the suprathreshold excitation of the posterior pulse (the broken curve), the preceding pulse evokes the excitation of the posterior pulse. (c) The preceding pulse suppresses the excitation of the posterior pulse when these positions are mismatched.

$$\mathbb{T} = \{ t_i | [u_{A_e}(t_i) = u_c] \wedge [du_{A_e}(t_i)/dt > 0] \},$$

where $u_c=0.5$ is a threshold parameter. The set of ISIs $\mathbb{S}$ is calculated from the time difference between the successive excitations:

$$\mathbb{S} = \{ s_i | s_i = t_{i+1} - t_i, t_i \in \mathbb{T} \}. \quad (7)$$

The probability as a function of the time interval between adjacent excitations, $P(s)$, is called the ISI distribution, and is often used to characterize neural activities [30]. In Fig. 9, the ISI distributions normalized by t_s are plotted for the signal-distributor and the propagation-block phases after an initial transient dies out, i.e., for $i \gg 1$. Here, we show the ISI distribution series in order to show the repetitive period dependency. In the case of the signal-distributor phase, the ISI distributions are unimodal functions, and the time interval for the maximum is unity for larger t_s values [see Fig. 9(a)]. This indicates that output nodes are excited by every external stimulus. In contrast, the ISI distributions are multimodal for the propagation-block phase. Further, the ISI takes discrete values, that is, integral multiples of the external period. This means that the trifurcated network acts as a band-pass filter, that is, the output nodes fire only for specific repetition-

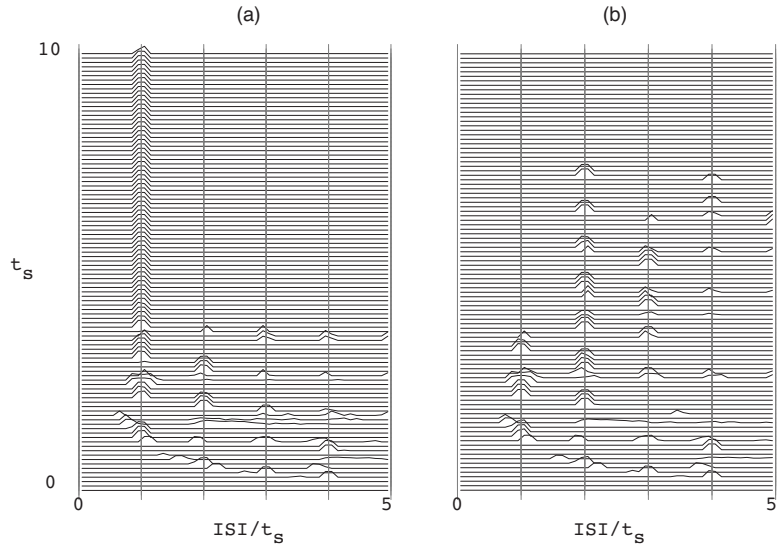

FIG. 9. Sequences of the normalized ISI distributions are shown as a function of the repetition period t_s. (a) The signal-distributor phase, $\alpha=0.002$. For larger t_s, the distributions are unimodal, and the probability takes a maximum when ISI equals t_s. (b) The propagation-block phase, $\alpha=0.003$. The distributions are multimodal, and each peak appears in the vicinity of integral multiples of the external period.

period regions. This recovery of signal transmission, which we have observed in the propagation-block phase, occurs in the following manner. After a pulse generated by a stimulus vanishes at the branch point, the state values of the elements in the vicinity of the branch point, u_i and v_i for $i \in \{O,1,2,3\}$, oscillate in time. If the posterior pulse arrived at the branch point in a certain time frame, during which u_O takes a larger value than some positive threshold, the oscillation of the branch-point element results in transmission to the output nodes.

In order to observe the relation between the input and output signals, we calculate the correlation function

$$c(\tau) = \overline{[u_{A_e}(t) - \overline{u_{A_e}(t)}][u_{C_e}(t-\tau) - \overline{u_{C_e}(t-\tau)}]} \Big/ \left(\sqrt{\overline{[u_{A_e}(t) - \overline{u_{A_e}(t)}]^2}}\sqrt{\overline{[u_{C_e}(t-\tau) - \overline{u_{C_e}(t-\tau)}]^2}}\right),$$

where $\overline{x(t)} = [\int_0^T x(t)dt]/T$ represents averaging over a long time for a given variable x (note that u_{A_e} and u_{C_e} are state variables of the input and output nodes, respectively). $c(\tau)$ is an oscillatory decreasing function and takes a maximum at a finite $\hat{\tau}$ due to the time delay between the input and output signals. Hence, we estimate the maximum of the correlation function $\hat{c} = |c(\hat{\tau})| = \max_\tau |c(\tau)|$ as a measure of the correlation between the input and output signals. In Fig. 10, the maximum is shown as a function of the repetition periods. The correlation is approximately 1 for a larger repetition period of the signal-distributor phase, i.e., the output nodes almost always respond with regard to longer repetition periods [Fig. 10(a)]. For a shorter repetition period, however, the maximum correlation takes a smaller value resulting from propagation failure due to inhibitory interaction between successive pulses, as is schematically shown in Fig. 8(c). In the case of the propagation-block phase, on the other hand, the maximum correlation takes a higher value in some regions, where signal transmission is recovered by the excitatory interaction between successive pulses. These observations are consistent with those in the SRR shown in Figs. 6(a) and 6(b).

Briefly, most of the pulses generated by inappropriate repetition periods annihilate at the branch point in the case of the distributor phase, and the signals generated by suitable repetition periods are transmitted to the output nodes in the case of the propagation-block phase. A correlation emerges between input and output excitations in these parameter regions, even if a single impulsive stimulus does not cause any

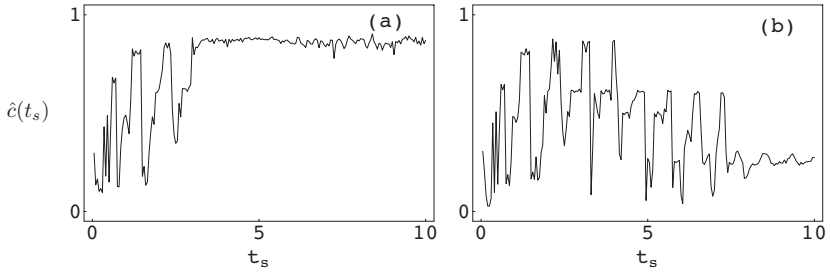

FIG. 10. Maximum correlation as a function of the repetition period. (a) The signal-distributor phase, $\alpha=0.001$. For larger t_s, the maximum correlation is approximately equal to 1, meaning that the output node almost always responds to the periodic stimulation. (b) The propagation-block phase, $\alpha=0.003$. The output nodes only respond to specific repetition periods.

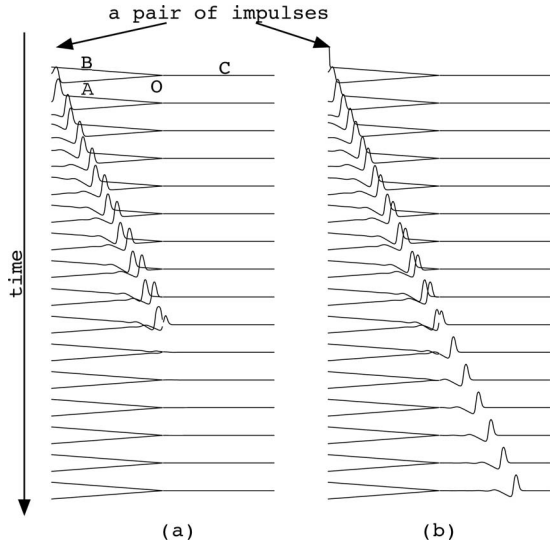

FIG. 11. Sequences of snapshots of the spatial pattern of $u_i(t)$. The input nodes A_e and B_e are excited at $t=0$ and $t=t_{lag}$, i.e., the two nodes are stimulated with a time lag t_{lag}. (a) $t_{lag}=1.0$; for longer time lags, the signals are blocked at the branch point. (b) $t_{lag}=0.03$; when the time lag between the stimuli is short, the signal can transfer to the daughter cable.

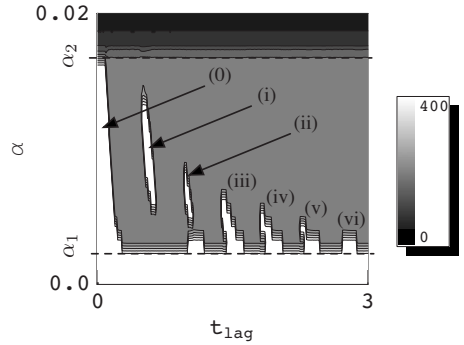

FIG. 12. Contour plot of signal propagation distance D in (t_{lag},α) parameter space. The pair of impulses is applied to the terminal nodes A_e and B_e with a time lag t_{lag}. White regions correspond to $D=400$, i.e., the complete propagation of the successive pulses. The gray region $\alpha_1<\alpha<\alpha_2$ corresponds to $D=200$ (the propagation block). Although the solitary pulse is blocked at the branch point as shown in Fig. 3(b), the pair of input signals is transferred to the output node when the time lag between them is sufficiently short. Furthermore, for a longer time lag, there are isolated white regions, i.e., $t_{lag}\in[2.05,2.1]$, [2.9,2.95], and [3.65,3.7] indicated by (0), (i), (ii), …, (vi), in which the signal transmission is recovered.

excitation of output nodes. These results indicate that the system performs similarly to band-pass and band-stop filters, depending on its parameters.

D. Response to a pair of impulses

In this section, we investigate the response to a pair of impulses with a time lag t_{lag}, each of which is applied to two different terminal nodes A_e and B_e. Here, we consider the following pair of impulses, i.e., we specify the state values of these input nodes by the following equations:

$$u_{3N-2}(0) = u_0,$$

$$v_{3N-2}(0) = v_0,$$

$$u_{3N-1}(t_{lag}) = u_0,$$

$$v_{3N-1}(t_{lag}) = v_0. \tag{8}$$

As we have seen, the solitary pulse generated by the single impulsive stimulus cannot surmount the branch point as in the propagation-block phase, i.e., $\alpha=0.002$. Even in this situation, however, applying the pair of impulses at two different terminals leads to the transmission of the signal beyond the branch point.

When the time lag between the pair is sufficiently large, the two pulses generated at $t=0$ and $t=t_{lag}$ cannot surmount the branch point (each pulse is blocked at the branch point, which means that the two pulses do not interact and each pulse behaves like a solitary pulse generated by a single impulse). The spatiotemporal behavior is shown in Fig. 11(a).

In Fig. 11(b), the series of spatial patterns for the recovery of propagation due to a pair of impulses with a smaller time lag is depicted. For shorter time lags, two pulses propagating from the parent cables arrive at the branch point synchronously, or nearly so (with a time lag t_{lag}). Thus, the state values of the two nodes connected to the branch point, (u_1,v_1) and (u_2,v_2), are nearly identical. Remember that the propagation block is a result of the effective increase of diffusivity due to the existence of three neighboring nodes at the branch point. The synchronous arrival (head-on collision) at the branch point reduces the diffusion of u effectively. This implies that the pulses behave as if they propagate in a normal cable whose elements have two neighboring nodes. Thus, the pulses surmount and propagate continuously against the effect of inhomogeneity, although there is a tiny time delay at the branch point. These results show that the Y-junction excitable cable functions as a coincidence detector in the following sense. The input signals can transfer to the output node, only if the two pulses enter the branch point synchronously, or nearly so.

In Fig. 12, the signal-propagation distance D defined by Eqs. (4) is plotted in (t_{lag},α)-parameter space. In the transient-propagation phase $\alpha>\alpha_2$, both pulses produced by the pair of impulses cannot reach the branch point, and thus D is less than 200. In the signal-distributor phase $\alpha<\alpha_1$, each input impulse leads to the excitation of the output node for any t_{lag}. In the propagation-block phase $\alpha_1<\alpha<\alpha_2$ in Fig. 12; however, most pulses vanish at the branch point (the gray region in $\alpha_1<\alpha<\alpha_2$ corresponds to the occurrence of the propagation block). As previously noted, the recovery of signal transmission is clearly recognized in the case of the pair of input impulses with shorter time lags, i.e., $t_{lag}\in[0.0,0.4]$ [white region indicated by (0) in Fig. 12]. Furthermore, the signals can also be transmitted to the output node in the isolated white regions, i.e., $t_{lag}\in[2.05,2.1]$, [2.9,2.95], and [3.65,3.7] in Fig. 12 indicated by (i), (ii), …,

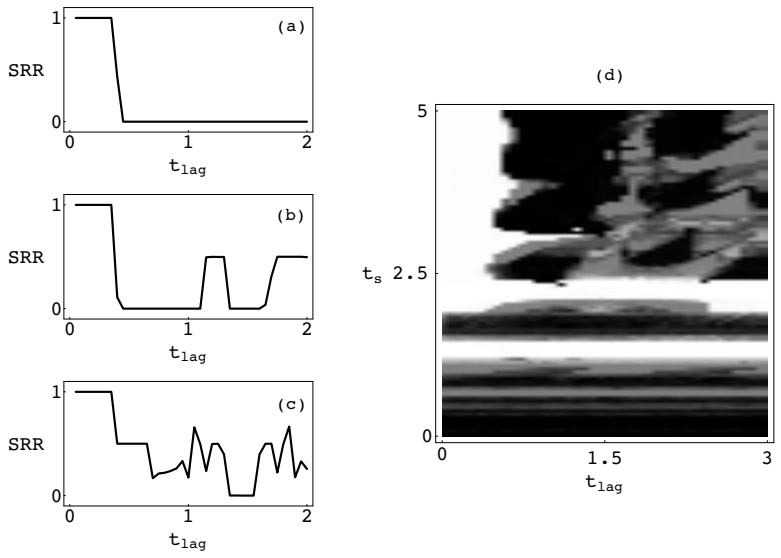

FIG. 13. SRR as a function of the time lag between the pair of impulses for the propagation-block phase, $\alpha=0.005$. A pair of impulses is applied periodically to the nodes A_e and B_e with a time lag t_{lag}. (a) $t_s=5.0$: input signals with a longer interval are transferred to the output node when $t_{lag}<0.45$ although the solitary pulse is blocked at the branch point, as shown in Fig. 3(b). (b) $t_s=2.2$: when the repetition period has intermediate values, positive SRR regions, $t_{lag}\in[1.05,1.3]$ and $[1.7,2.0]$, appear. The SRR is approximately equal to 1/2. (c) $t_s=1.45$: there are unsteady regions $t_{lag}\in[0.8,3]$ and $[1.5,2.0]$ where the signals are transmitted to the output node irregularly. (d) The SRR in (t_{lag},t_s) is shown by a gray scale; the maximum value of 1.0 corresponds to white, and the minimum value 0.0 to black.

(vi), where D equals 400. These regions originate from the coordination between the suprathreshold pulse generated at $t=t_{lag}$ and the subthreshold humps arising after the disappearance of the pulse generated at $t=0$. Thus, the recovery of transmission occurs if the time lag t_{lag} is approximately equal to the integral multiples of the oscillation period, i.e., an intrinsic period t_λ, that can be estimated as follows. The intrinsic period originates from the period of the oscillating wake of the traveling pulse. This oscillation can be determined by the eigenvalues of the uniform stationary solution $(u,v)=(0,0)$, which are given by

$$\lambda_\pm=[-\alpha-\gamma\tau\pm\sqrt{-4(1+\alpha\gamma)\tau+(\alpha+\gamma\tau)^2}]/(2\tau).$$

Therefore, the intrinsic period is given by

$$t_\lambda=2\pi/|\mathrm{Im}(\lambda)|, \tag{9}$$

where $\mathrm{Im}(\cdot)$ represents the imaginary part [10].

The dynamics of the recovery of the pulse transmission is outlined as follows. After the suprathreshold excitation (generated by the impulse at $t=0$) disappears at the branch point, the state value u of the nodes in the neighborhood of the branch point oscillates due to the wake. When the posterior pulse arrives at the branch point within a certain time interval, during which u_0 takes a positive value larger than a certain threshold value, it surmounts the branch point. In other words, the posterior pulse entering the branch point can surmount it only with the aid of the aftereffect of the disappearance of the preceding pulse. Thus, whether the signals are transmitted to the output node depends crucially on the time lag between the pair of impulses. The isolated white regions in Fig. 12 indicated by (i), (ii), …, and (vi) correspond to the recoveries of signal transmission by the assistance of the first, second, …, and sixth subthreshold humps, respectively.

E. Response to the repetition of the pair of impulses

The spatiotemporal behavior in response to the pair of periodic stimulations depends on the time lag t_{lag} and the repetition period t_s. The pair of impulses is applied to two nodes A_e and B_e instantaneously, that is, the state values of the two nodes u_{A_e} and u_{B_e} are specified by the following equations:

$$u_{3N-1}(t_i)=u_0,$$

$$u_{3N-2}(t_i-t_{lag})=u_0,$$

$$v_{3N-1}(t_i)=v_0,$$

$$v_{3N-2}(t_i-t_{lag})=v_0, \tag{10}$$

where $t_i\in\mathcal{T}$ is an element of the set of time defined in Eqs. (6). Here, we examine the effect of the repetition for the propagation-block phase.

To observe the (t_s,t_{lag})-parameter dependence of input-output relation, we calculate the SRR as a function of t_{lag} for three different values of the repetition period, i.e., $t_s=5.0$, 2.2, and 1.45. The parameter dependency for the propagation-block phase is depicted in Fig. 13. When the repetition period t_s is larger, the transmission property of pulse trains generated by the repetition of the pair impulses does not change. The recovery of the pulse propagation occurs only for a smaller time lag between the pair of impulses [see Fig. 13(a)]. This is because the branch-point oscillation after the disappearance of the pulse decays before the succeeding pulses arrive. The input-output relationship in the case of the repetition of the pair impulses is essentially the same as that in the case of the single pair of impulses discussed in the previous section—if the time lag between the pair is shorter than a critical value, i.e., $t_{lag}<0.45$, all the pulses generated by the repetition of the pair of impulses are transferred to the output node; otherwise, they are blocked at the branch point.

However, the repetition of the pair of impulses with a shorter t_s results in the propagation of pulses beyond the branch point, which is clearly observed as positive SRR regions for $t_{lag}>0.45$ in Figs. 13(b) and 13(c). When the repetition period becomes shorter, a complex structure emerges.

This occurs in the following manner. After the first pair of pulses annihilates at the branch point, subthreshold oscillation occurs in the neighborhood of the branch point owing to the oscillatory wake, as described in the previous section. This subthreshold oscillation stimulates the subsequent pulse to surmount the branch point. When the arrival time of the subsequent pulse at the branch point coincides with the time at which u becomes larger than a certain threshold value, the subthreshold oscillation acts as a stimulant for surmounting the branch point.

In Fig. 13, the plateaus at a value close to a rational number show the locking state between input and output signals. Furthermore, the unsteady regions observed in Fig. 13(c) of the SRR indicate a chaotic (unlocked) state that is a result of the nonlinear interaction between the aftereffect of the vanished pulse and the subsequent pulse entering the branch point. An irregular time series of output signals is observed in this unlocked state, and whether the pulse surmounts the branch point crucially depends on the history of the previous pulse.

F. Response to aperiodic impulses

In this section, we analyze the effects of the fluctuation of the repetition period on the input-output relationship. Aperiodic impulses are applied to the two terminals A_e and B_e. Here, we introduce the fluctuation (or irregularity) of input signals as follows:

$$u_{A_e}(t_i + \xi_i) = u_0,$$

$$u_{B_e}(t_j + \xi_j + t_{lag}) = u_0,$$

$$v_{A_e}(t_i + \xi_i) = v_0,$$

$$v_{B_e}(t_j + \xi_j + t_{lag}) = v_0,$$

where t_i and t_j are elements of the time sequence defined in Eqs. (6), and the fluctuation ξ_i is assumed to be Gaussian white noise of zero mean:

$$P(\xi_i) = \frac{1}{\sqrt{2\pi\sigma^2}} \exp\left(-\frac{\xi_i^2}{2\sigma^2}\right), \tag{11}$$

where σ determines the variance of the fluctuation of the repetition period. It is also assumed that the noise ξ_i and ξ_j are independent:

$$\langle \xi_i \xi_j \rangle = \delta_{i,j}, \tag{12}$$

where $\delta_{i,j}$ is Kronecker's delta.

We calculate the ISI distribution defined in Eq. (7) so as to characterize the effect of the fluctuation statistically. After an initial transient died out, i.e., for $i \gg 1$, the ISI distributions for different values of the variance σ of the Gaussian noise for $t_s=5.0$ are plotted in Fig. 14. When the variance of the fluctuation is small, the parameter used here shows the situation in which the input-output signal ratio is locked to 1:1 and the corresponding SRR equals 1. Thus, the ISI takes the same value of the repetition period, i.e., $t_s=5.0$. When the variance increases, the ISI fluctuates, and the single peak in the ISI distribution at $t_s=5.0$ broadens. As the variance increases further, i.e., σ decreases, a new peak eventually appears in the ISI distribution. One can see that multimodal distribution is obtained as shown in Figs. 14(a) and 14(b). For smaller σ, each peak in the ISI distribution is approximately Gaussian. Finally, by increasing the variance of the fluctuation, i.e., decreasing σ, we observe that each Gaussian distribution is broadened further, and a unimodal distribution is formed as depicted in Fig. 14(c). This means that, although the time intervals between input impulses t_s are 5.0, ISIs in response to the aperiodic input impulses often take very large values compared to those in response to a periodic one. The ISI distribution for smaller σ is approximately exponential for longer ISIs. However, for shorter intervals, there is a rapid decrease in the distribution, reflecting the fact that neurons are refractory immediately after excitation.

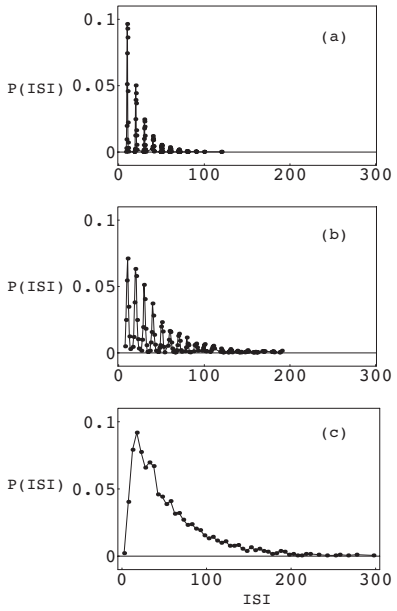

FIG. 14. ISI distributions for different values of the variance of the fluctuation. The distribution is multimodal for smaller σ, and each peak region is approximately of the Gaussian form. With increase in the variance of the fluctuation, these Gaussian peaks become a unimodal distribution. $\sigma^2=$ (a) 0.1, (b) 0.25, and (c) 0.5. $t_{lag}=0.1$, $t_s=5.0$, and the other parameters are the same as in Fig. 13.

In Fig. 15, the ISI distributions of the input and the output nodes are shown for $t_{lag}=0$. Although the mean time lag between the pair of impulses is zero, there will be a time delay between the arrival times of pulses propagating from the two terminals due to the effect of the fluctuation ξ. It can be seen that the standard deviation of the ISI distribution at the output node is smaller than σ when the repetition period is in the neighborhood of integral multiples of the intrinsic period t_λ [see Fig. 15(a)]. In other words, the detection of coincidence by the trifurcated nerve system is robust against noisy input signals. When the mean repetition period has intermediate values, i.e., the stimulation intervals are in the region of $(n+1/2)t_\lambda$, the ISI distribution at the output node is multimodal as depicted in Fig. 15(b). Each peak corresponds

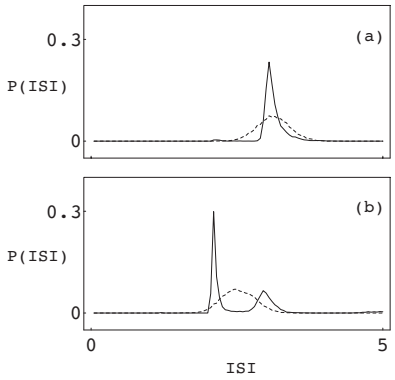

FIG. 15. ISI distributions for different values of the repetition period. The solid and broken lines indicate the ISI distribution measured at the output node and the input node, respectively. (a) $t_s=3.1$: the standard deviation of the ISI distribution obtained at the output node is smaller than that at the input nodes. (b) $t_s=2.5$: the ISI distribution of the output element is multimodal and consists of two Gaussian peaks. The variances of each peak are smaller than that of the unimodal ISI distribution measured for the input elements. $\sigma=5.0$ and $t_{lag}=0$. The other parameters are the same as in Fig. 13.

to integral multiples of the intrinsic period t_λ in Eq. (9). Further, the ISI distribution is approximately assembled from the two Gaussian distributions, each of which has a smaller variance than that of the original input signals. In both cases, the ISI distribution measured at the output node has a sharper peak than that at the input nodes. This means that the fluctuation in ISIs at the output node is reduced through the interaction of pulses at the branch point.

IV. SUMMARY

We have studied the spatiotemporal dynamics of pulse propagation in FHN excitable elements, which are arranged to form a trifurcated structure, i.e., a Y-junction cable. Each element connects diffusively, and the Kirchhoff law holds at each node. We have investigated the pulse dynamics responding to four types of stimulation pattern: (a) single impulsive stimulation, which is applied to one of the terminal nodes, (b) a pair of single impulses with time delay, which is applied to two terminals of the cables, (c) repetitive stimulation at one of the terminals, and (d) repetitive stimulation of the pair of impulses.

A. Single stimulus

When we apply a single impulse at one of the cable terminals, a pulse forms and propagates in the father cable, i.e., the cable at which the terminal node is excited. We have found the following three phases for the spatiotemporal behaviors on changing the excitability of an element, the parameter α.

(i) *Signal distributor*. When the excitability of each element is higher than $\alpha_1 \simeq 0.0028$, the pulse generated by the single impulse propagates in the father cable and reaches the branch point (the junction of three cables). At the branch point, the pulse splits into two pulses, each of which propagates in two daughter cables. In this case, the chain of excitable elements arranged in the shape of a trifurcated structure acts as a signal distributor.

(ii) *Propagation block*. For intermediate values of α, $\alpha_1 < \alpha < \alpha_2 \simeq 0.017$, the pulse propagating in the father cable is blocked at the branch point. The pulse disappears at the branch point because the existence of three neighboring nodes increases the diffusion of the activator.

(iii) *Transient propagation*. When the excitability of the element is much lower, $\alpha > \alpha_2$, the pulse propagates transiently in the father cable, and eventually vanishes before it reaches the branch point. This transition is a result of the disappearance of a stable traveling pulse solution through the saddle-node bifurcation.

B. Repetition of a single stimulus

The repetition of a single impulse shows exotic spatiotemporal behaviors through an interaction between previous and posterior pulses generated by successive stimuli. In particular, the repetition of a single impulse leads to the surmounting of the branch point even in the propagation-block phase. The signal transmission is recovered when the repetition period takes only specific values. For a signal distributor, all signals are transmitted to the output nodes when the repetition period is sufficiently large. However, the signals are blocked for some specific values of the repetition period. These phenomena are caused by the interaction between successive pulses generated by the repetitive stimulation. The repetition period plays a crucial role in determining the recovery and failure of signal transmission in the propagation-block and signal-distributor phases, respectively. The output elements are excited or inhibited depending on the repetition period, and thus the system acts as a band-pass or band-stop filter for the repetitive input signals.

C. Pair of stimuli with a delay

We have studied statistics of the output signal when a pair of stimuli are applied to two different terminals of cables in the propagation-block phase. Due to the collision between pulses originating from different sources, whether these pulses can surmount the branch point depends crucially on the time lag between the input impulses. The behaviors for longer time lags are analogous to those observed in the case of the single impulse; the two pulses generated by the pair of stimulations disappear at the branch point. However, the pair of impulses with shorter time lags results in a pulse collision at the branch point, and it leads to the recovery of signal transmission. The Y-junction cable act as a coincidence detector in the propagation-block phase.

Furthermore, the recovery is also observed in the case of suitable delays that are integral of multiples of the intrinsic period of FHN elements. This recovery of signals with a larger delay is caused by the interaction between successive pulses entering the branch point in the following manner. After the preceding pulse disappears at the branch point (here, we consider the propagation-block phase), the excitable element at the branch point relaxes into a rest state, and

this relaxation dynamics is a damped oscillation that can be attributed to the existence of imaginary parts of the eigenvalues for the rest state. As a result, this oscillation produces an inhibitory or excitatory interaction with the posterior pulse depending on the time delay between the pair of stimuli. If the arrival time of the posterior pulse at the branch point is a term that can be defined as the duration for the value of the activator u_O to become larger than a certain threshold value, the propagation is recovered by the aftereffect of the disappearance of the preceding pulse.

D. Repetition of a pair of stimuli

The relationship between the input and output signals is also influenced by the repetition of the pair of impulses. When the time lag between the pair of stimuli and the repetition period is sufficiently large, all pulses vanish near the branch point for the propagation-block phase. However, the repetition of the pair of impulses with suitable periods allows the transmission of signal to the output node again, and this recovery of signal transmission is a result of the aftereffect of vanished pulse at the branch point. The interaction between successive pulses in a cable and the aftereffect of the vanished pulse produces more complex spatiotemporal behaviors, i.e., behaviors such as the transmission recovery, propagation block, input-output signal locking phenomena, and irregular excitation of output elements emerge, depending on the time delay and repetition period.

E. The effect of aperiodicity

We have also studied the response to aperiodic input impulses. The aperiodicity considered here is that both the time lags t_{lag} and the repetition period t_s fluctuate independently in the vicinity of their mean values. When the fluctuation is smaller, the ISI distribution has a sharp peak at the mean value of the repetition period if the delay between the pair of impulses is sufficiently short. As the fluctuation increases, a new peak appears in the ISI distribution, and the number of the peaks gradually increases. Each peak is approximately Gaussian, and it gradually broadens with increasing fluctuation. These Gaussian peaks finally connect to form a unimodal distribution that has an exponential tail for larger ISIs and has a rapid decrease for shorter ISIs

For a pair of stimuli with varying repetition periods and time delays, the variance of ISI distribution measured at the output node is reduced; the variance of the ISI distribution at the output node is smaller than that at the input nodes. When a simple Y-junctioned cable collects afferent inputs from multiple sources, it acts as a fluctuation reducer.

Finally, it is noteworthy that the complex shapes of neurons might play an important role during signal processing. The results of the above discussion illustrate some aspects of the nerve cell as the basis for the integration of information originating from different sources. The neuromorph (a simple Y-junctioned cable) responds to particular combinations of input patterns in time and space. The study of these dynamics is of general application in the understanding of disordered phenomena in spatially extended excitable media, and it might provide new insight into excitable systems such as neural dynamics.

ACKNOWLEDGMENTS

This research was partially supported by the Ministry of Education, Science, Sports and Culture of Japan, Grant-in-Aid for Scientific Research No. 19540390.

[1] A. I. Hodgkin and A. F. Huxley, J. Physiol. **117**, 500 (1952).
[2] R. FitzHugh, J. Gen. Physiol. **43**, 867 (1960).
[3] J. Nagumo, S. Arimoto, and S. Yoshizawa, Proc. IRE **50**, 2061 (1962).
[4] R. D. Chialvo and J. Jalife, Nature (London) **330**, 749 (1987).
[5] L. Glass, Nature (London) **410**, 277 (2001).
[6] V. A. Makarov, V. I. Nekorkin, and M. G. Velarde, Phys. Rev. Lett. **86**, 3431 (2001).
[7] T. Nomura and L. Glass, Phys. Rev. E **53**, 6353 (1996).
[8] M. Courtemanche, L. Glass, and J. P. Keener, Phys. Rev. Lett. **70**, 2182 (1993).
[9] Y. Nagai, H. González, A. Shrier, and L. Glass, Phys. Rev. Lett.. **84**, 4248 (2000).
[10] T. Yanagita, Y. Nishiura, and R. Kobayashi, Phys. Rev. E **71**, 036226 (2005).
[11] H. Agmon-Snir, C. E. Carr, and J. Rinzel, Nature (London) **393**, 268 (1998).
[12] C. Koch and I. Segev, Nat. Neurosci.. **3**, 1171 (2000).
[13] I. Segev and E. Schneidman, J. Physiol. **93**, 263 (1999).
[14] I. Segev and M. London, Science **290**, 744 (2000).
[15] W. Rall, in *Neural Theory and Modeling*, edited by R. F. Reiss (Stanford University Press, Stanford, CA, 1964), pp. 73–97.
[16] *The Theoretical Foundations of Dendritic Function: Selected Papers of Wilfrid Rall with Commentaries*, edited by I. Segev, J. Rinzel, and G. M. Shepherd (MIT Press, Cambridge, MA, 1995).
[17] I. Segev and W. Rall, Trends Neurosci. **21**, 453 (1998).
[18] Y. Manor, C. Koch, and I. Segev, Biophys. J. **60**, 1424 (1991).
[19] D. Debanne, Nat. Rev. Neurosci. **5**, 304 (2004).
[20] T. Yanagita, Y. Nishiura, and R. Kobayashi, Prog. Theor. Phys. Suppl. **161**, 393 (2006).
[21] E. Yanagida, Jpn. J. Ind. Appl. Math. **18**, 25 (2001).
[22] R. FitzHugh, Biophys. J. **1**, 445 (1961).
[23] E. Meron, Phys. Rep. **218**, 1 (1992).
[24] J. Rinzel and J. Keller, Biophys. J. **13**, 1313 (1973).
[25] G. Matsumoto, K. Aihara, Y. Hanyu, N. Takahashi, S. Yoshizawa, and J. Nagumo, Phys. Lett. A **123**, 162 (1987).
[26] A. T. Winfree, Physica D **49**, 125 (1991).
[27] K. J. Lee, Phys. Rev. Lett. **79**, 2907 (1997).
[28] O. Steinbock, Phys. Rev. Lett. **88**, 228302 (2002).
[29] H.-M. Liao, L.-Q. Zhou, C.-X. Zhang, and Q. Ouyang, Phys. Rev. Lett. **95**, 238301 (2005).
[30] J. R. Clay, J. Comput. Neurosci. **15**, 43 (2003).